Technical Note

Effects of Ilmenite on the Properties of Microwave-Sintered Lunar Regolith Simulant

Chuanjiao Zhou[1]; Hong Tang[2]; Xiongyao Li[3]; Xiaojia Zeng[4]; Wen Yu[5]; Bing Mo[6]; Rui Li[7]; Jianzhong Liu[8]; and Yongliao Zou[9]

Abstract: Microwave sintering is regarded as a high-efficiency, energy-saving, and rapid-heating technique for the preparation of structural materials on the Moon. However, the influencing factors (i.e., ilmenite content and sintering temperature) on microwave sintering processes are not well-understood. Herein, five lunar regolith simulants with different contents of ilmenite (i.e., 4.6%, 28.5%, 43.9%, 65.8%, and 80.9% by weight) were used for microwave sintering experiments at 1,050°C, 1,150°C, and 1,300°C. The characterization of the microstructure, mineralogy, thermal conductivity, and mechanical properties of the products shows that the ilmenite content and sintering temperature significantly affected the properties of the microwave-sintered products. The sintering product containing 4.6% by weight ilmenite at 1,300°C showed a dense texture, good thermal insulation properties (thermal conductivity of 0.15 ± 0.005 W m^{-1} K^{-1}), and optimal compressive strength (74.0 ± 7.1 MPa). This suggests that adding ilmenite to lunar regolith does not improve the properties of microwave-sintered products. The results in this paper provide reference for the preparation of structural materials on the Moon in the future. **DOI: 10.1061/(ASCE)AS.1943-5525.0001344.** © *2021 American Society of Civil Engineers.*

Author keywords: Microwave sintering; Lunar regolith; In situ resource utilization (ISRU); Structural material.

Introduction

Utilizing lunar resources and establishing lunar bases are the primary objectives of lunar exploration in the 21st century (Rousek et al. 2012; Kalapodis et al. 2020). A lunar base requires a significant amount of structural material, but transportation of these materials from the Earth to the Moon is notably expensive (Duke et al. 2003). The lunar surface is covered with a layer (1–10 m in thickness) of fine-grained regolith, formed by long-time impacts of meteorites and micrometeorites, exposure to cosmic rays and solar wind, and thermal cycling. Mineralogically, lunar regolith is mainly composed of rock chips, mineral particles, glass fragments, and highly porous agglutinates (Lucey et al. 2006; Crawford 2015). Importantly, basaltic regolith commonly contains ~1.9% to 23.9% by weight ilmenite (Sato et al. 2017). Lunar regolith is a preferred material for in situ resource utilization (ISRU) on the Moon (Ruess et al. 2006; Faierson and Logan 2012; Lim et al. 2017; Zhou et al. 2019).

To prepare the structural materials for lunar bases, a wide range of techniques has been investigated, including electrothermal sintering (Allen et al. 1992; Altemir et al. 1993; Song et al. 2020), laser sintering (Balla et al. 2012; Fateri et al. 2013; Fateri and Gebhardt 2015), solar sintering (Cardiff and Hall 2008; Nakamura and Smith 2005; Fateri et al. 2019), microwave sintering (Wright et al. 1986;

[1]Graduate Student, Center for Lunar and Planetary Sciences, Institute of Geochemistry, Chinese Academy of Sciences, Guiyang 550081, China; College of Earth and Planetary Sciences, Univ. of Chinese Academy of Sciences, Beijing 100049, China. Email: zhouchuanjiao@mail.gyig.ac.cn

[2]Professor, Research Fellow, Center for Lunar and Planetary Sciences, Institute of Geochemistry, Chinese Academy of Sciences, Guiyang 550081, China; CAS Center for Excellence in Comparative Planetology, Hefei 230026, China; Key Laboratory of Space Manufacturing Technology, Chinese Academy of Sciences, Beijing 100094, China (corresponding author). Email: tanghong@vip.gyig.ac.cn

[3]Professor, Research Fellow, Center for Lunar and Planetary Sciences, Institute of Geochemistry, Chinese Academy of Sciences, Guiyang 550081, China; CAS Center for Excellence in Comparative Planetology, Hefei 230026, China; Key Laboratory of Space Manufacturing Technology, Chinese Academy of Sciences, Beijing 100094, China. Email: lixiongyao@mail.gyig.ac.cn

[4]Postdoctor, Center for Lunar and Planetary Sciences, Institute of Geochemistry, Chinese Academy of Sciences, Guiyang 550081, China; Key Laboratory of Space Manufacturing Technology, Chinese Academy of Sciences, Beijing 100094, China. Email: zengxiaojia@mail.gyig.ac.cn

Note. This manuscript was submitted on January 21, 2021; approved on June 29, 2021; published online on August 10, 2021. Discussion period open until January 10, 2022; separate discussions must be submitted for individual papers. This technical note is part of the ***Journal of Aerospace Engineering***, © ASCE, ISSN 0893-1321.

[5]Technical Engineer, Center for Lunar and Planetary Sciences, Institute of Geochemistry, Chinese Academy of Sciences, Guiyang 550081, China; CAS Center for Excellence in Comparative Planetology, Hefei 230026, China; Key Laboratory of Space Manufacturing Technology, Chinese Academy of Sciences, Beijing 100094, China. Email: yuwen@mail.gyig.ac.cn

[6]Technical Engineer, Center for Lunar and Planetary Sciences, Institute of Geochemistry, Chinese Academy of Sciences, Guiyang 550081, China; CAS Center for Excellence in Comparative Planetology, Hefei 230026, China; Key Laboratory of Space Manufacturing Technology, Chinese Academy of Sciences, Beijing 100094, China. Email: mobing@mail.gyig.ac.cn

[7]Technical Engineer, Center for Lunar and Planetary Sciences, Institute of Geochemistry, Chinese Academy of Sciences, Guiyang 550081, China; CAS Center for Excellence in Comparative Planetology, Hefei 230026, China; Key Laboratory of Space Manufacturing Technology, Chinese Academy of Sciences, Beijing 100094, China. Email: lirui@mail.gyig.ac.cn

[8]Research Fellow, Center for Lunar and Planetary Sciences, Institute of Geochemistry, Chinese Academy of Sciences, Guiyang 550081, China; CAS Center for Excellence in Comparative Planetology, Hefei 230026, China; Key Laboratory of Space Manufacturing Technology, Chinese Academy of Sciences, Beijing 100094, China. Email: liujianzhong@mail.gyig.ac.cn

[9]Research Fellow, National Space Science Center, Chinese Academy of Sciences, Beijing 100190, China. Email: zouyongliao@nssc.ac.cn

Downloaded from ascelibrary.org by TSINGHUA UNIVERSITY on 11/28/21. Copyright ASCE. For personal use only; all rights reserved.

Meek et al. 1987), and three-dimensional (3D) printing (Ceccanti et al. 2010; Taylor et al. 2018; Xu et al. 2019). Among these techniques, microwave sintering has the unique advantages of high efficiency, even heating, and energy availability. First, compared with other sintering techniques, microwave sintering is energy-efficient (energy savings of 90%) and heats quickly. In addition, a large penetration of heat (13.4 mm depth for 2.45-GHz microwaves) can be achieved by microwave sintering (Lim et al. 2017, 2021). Second, even heating is inherent to microwave sintering because the heat is produced by coupling certain microwave frequencies with specific materials that uniformly absorb microwave energy (Taylor and Meek 2005). Third, because microwave energy is independent of sunlight, it is be readily available and easily obtained on the Moon (Lim et al. 2017). These facts make microwave sintering especially relevant in high-temperature sintering experiments on the Moon.

The application of microwave sintering on lunar regolith has been investigated for over 35 years. A series of microwave sintering experiments on terrestrial basalts with ilmenite have shown that ilmenite can promote the coupling between samples and microwaves (Wright et al. 1986; Meek et al. 1984; Vaniman et al. 1986; Hill et al. 2005). Meek et al. (1987) conducted microwave sintering experiments on three lunar regolith simulants, the results of which indicated that the compressive strength and hardness of the products varied greatly with different temperatures and compositions. Allen et al. (1994) and Allen (1998) performed microwave heating experiments on lunar regolith simulants JSC-1 and MLS-1, and the samples were uniformly sintered and crack-free. Temple et al. (2006) indicated that the powdered graphite in JSC-1 samples could promote a reduction reaction in microwave heating experiments. Taylor and Meek (2005) investigated the effect of nanophase-sized Fe^0 grains on microwave sintering of Apollo 17 lunar regolith. Specifically, the transient liquid phase created by nanophase Fe^0 could promote the melting of samples, which makes microwave sintering technology potentially applicable to sintering lunar regolith. Allan et al. (2013) modeled and conducted microwave processing of the JSC-1A lunar simulant. This study was based on the geometry of heating patterns, and various temperature ranges demonstrated a good representation of JSC-1A microwave-surface heating.

Previous studies demonstrated that microwave sintering can effectively solidify simulated lunar regolith. However, the factors affecting the microwave sintering process, such as ilmenite content and sintering temperature, are not well-understood. In this study, a series of microwave sintering experiments have on lunar regolith simulants with different ilmenite content at different sintering temperatures, with the aim to investigate the effects of ilmenite content and sintering temperature on the properties of microwave-sintered lunar regolith simulants.

Preparation of Regolith Simulants with Different Contents of Ilmenite

In this study, the low-titanium basaltic lunar regolith simulant CLRS-1 [also known as CAS-1 lunar regolith simulant (Zheng et al. 2009)] was used for microwave sintering. To prepare a series of lunar regolith simulants with different contents of ilmenite, the micrometer-sized (<100 μm) powders of terrestrial ilmenite concentrate (sourced from Panzhihua, Sichuan Province, China) were mixed with the CLRS-1 regolith simulant in various ratios (i.e., 1:0, 7:3, 1:1, 3:7, and 0:1) (Table 1). Bulk TiO_2 contents for these prepared five samples were characterized using X-ray fluorescence spectrometry (XRF) (ARL Perform'X Sequential XRF, Thermo Fisher Scientific, Waltham, Massachusetts) at the Institute of Geochemistry, Chinese Academy of Sciences, following standard procedures (e.g., Deng et al. 2017). Based on the TiO_2 content, the ilmenite content in each sample was calculated (i.e., 4.6%, 28.5%, 43.9%, 65.8%, and 80.9% by weight, respectively) (Table 1).

Table 1. Information on the studied samples and microwave sintering experiments

Samples	Components	TiO_2 (% by weight)	Contents of ilmenite[a] (% by weight)	Sintering temperature (°C)
1-1050	100% CLRS-1	2.42	4.6	1,050
1-1150				1,150
1-1300				1,300
2-1050	70%CLRS-1 + 30%	14.99	28.5	1,050
2-1150	ilmenite concentrate			1,150
2-1300				1,300
3-1050	50%CLRS-1 + 50%	23.12	43.9	1,050
3-1150	ilmenite concentrate			1,150
3-1300				1,300
4-1050	30%CLRS-1 + 70%	34.65	65.8	1,050
4-1150	ilmenite concentrate			1,150
4-1300				1,300
5-1050	100% ilmenite	42.59	80.9	1,050
5-1150	concentrate			1,150
5-1300				1,300

[a]Contents of ilmenite were calculated from the abundance of TiO_2 determined by XRF.

Microwave Sintering Experiments

Before microwave sintering experiments, the prepared regolith simulant with different ilmenite abundance were dried at the temperature of 120°C for 24 h. The five oven-dried samples were then placed in a rectangular alumina crucible with the dimensions of 60 × 30 × 30 mm [Figs. 1(a and b)]. Each sample was prepared (three groups of 25 g each) for the microwave sintering experiments in a microwave high-temperature furnace (CY-AT1700 C-M, Hunan change Microwave Technology, Changsha, China) at the Institute of Geochemistry, Chinese Academy of Sciences. This instrument is a controlled-atmosphere high-temperature sintering furnace heated by microwaves.

During the microwave sintering experiments, the samples were placed in alumina crucibles without compression and then put into the heating chamber of the microwave high-temperature furnace for sintering. This furnace was evacuated and then filled with flowing high-purity argon and 3%–4% nitrogen. The chamber of the furnace was maintained at 88,790 Pa (1 atmospheric pressure) during the entire sintering experiment. The sintering experiments for each sample were performed at temperatures of 1,050°C, 1,150°C, and 1,300°C, with a hold time of 1 h at the target temperature (Table 1). The heating rate was set as 6°C/min, and the power was 500–1,800 W. After the sintering experiment, the samples were cooled to 800°C by controlling the microwave power at a cooling rate of 6°C/min, followed by natural cooling. All temperatures mentioned here refer to the temperature in the chamber of the microwave high-temperature furnace.

Analytical Methods

The microstructure of sintered regolith simulant was observed using a FEI Scios dual-beam focused ion beam/scanning electron microscope (FIB/SEM, Thermo Fisher Scientific, Waltham, Massachusetts) at the Institute of Geochemistry, Chinese Academy of Sciences. The representative back-scattered electron (BSE) images

Downloaded from ascelibrary.org by TSINGHUA UNIVERSITY on 11/28/21. Copyright ASCE. For personal use only; all rights reserved.

of each sample were collected with the following conditions: 15 kV accelerating voltage, 0.2–0.8 nA beam current, 7 mm working distance, and ~50× magnification.

The phase composition of the samples before and after the sintering experiments were obtained by X-ray diffraction (XRD), with Ni-filtered and Cu radiation at 40 kV and 40 Ma, which was performed at the State Key Laboratory of Ore Deposit Geochemistry, Institute of Geochemistry, Chinese Academy of Sciences. Approximately 0.5 g of each sample was prepared and sent for testing after grinding and drying for 24 h.

The thermal conductivity of the samples before and after the sintering experiments was measured using a thermal analyzer (Hot Disk TPS2500S, Uppsala, Sweden) at the Institute of Geochemistry, Chinese Academy of Sciences. Approximately 20 g of powder sample before the sintering experiments was weighed and measured using a 5,501 probe with a radius of 6.403 mm. For the solid products after the sintering experiments, the samples were cut into 6–8 mm cubes and then measured using a 7,577 probe with a radius of 2.001 mm. All measurements were performed at ~20°C and a pressure of ~10 Pa for 1,280 s.

Compressive strength was measured using a microcomputer controlled electronic universal testing machine (BTM5105, Shenyang BAOTAK Instrument, Shenyang, China) with a maximum load of 100 kN, conducted at the Chongqing Institute of Green and Intelligent Technology, Chinese Academy of Sciences. Two regular cubes of each sample were prepared with lengths of 6–8 mm for the measurements. The displacement rate during the compression process was 0.5 mm/min.

Results and Discussion

All powder samples were solidified and shaped with some volume shrinkage after sintering. The appearances of the sintered products were black, with few visible cracks on their surface. Fig. 1 shows the sintered products cut by a computer-controlled diamond wire-cutting machine; the dimensions of the products were cubical with side lengths of 6–8 mm. Some small pores were observable in all cut products, with more pores in the products with low sintering temperature and high ilmenite content. To compare the influence of ilmenite content and sintering temperature on the properties of the sintered products, the characteristics of microstructure, mineralogy, thermal performance, and compressive strength of all products were analyzed.

Microstructures

Fig. 2 shows representative SEM images of the 15 sintered products, with different contents of ilmenite and sintering temperatures (i.e., 1,050°C, 1,150°C, and 1,300°C). The results indicate that all the sintered samples were either melted or recrystallized. Pores and cracks were observed in all products. However, the sizes and numbers of these pores and cracks varied with the ilmenite content and sintering temperature:

- As the ilmenite content increased, the pore sizes and the number of pores and cracks generally increased. This indicates that the difference in the microwave absorption capacity of ilmenite and silicate leads to different thermal effects during the microwave sintering process.
- As the sintering temperature increased, the pore size and number of pores decreased, except for the products from the samples with 80.9% by weight ilmenite. This suggests that a large amount of gas escaped below 1,200°C.
- The products from samples with 4.6% by weight ilmenite sintered at 1,300°C had a dense texture due to the advantages of uniformity and the presence of small pores and few cracks.

Mineralogy

Determination of mineralogy of sintered products was performed to assist in investigating the reaction in the samples during the microwave sintering. The XRD results showed that silicate

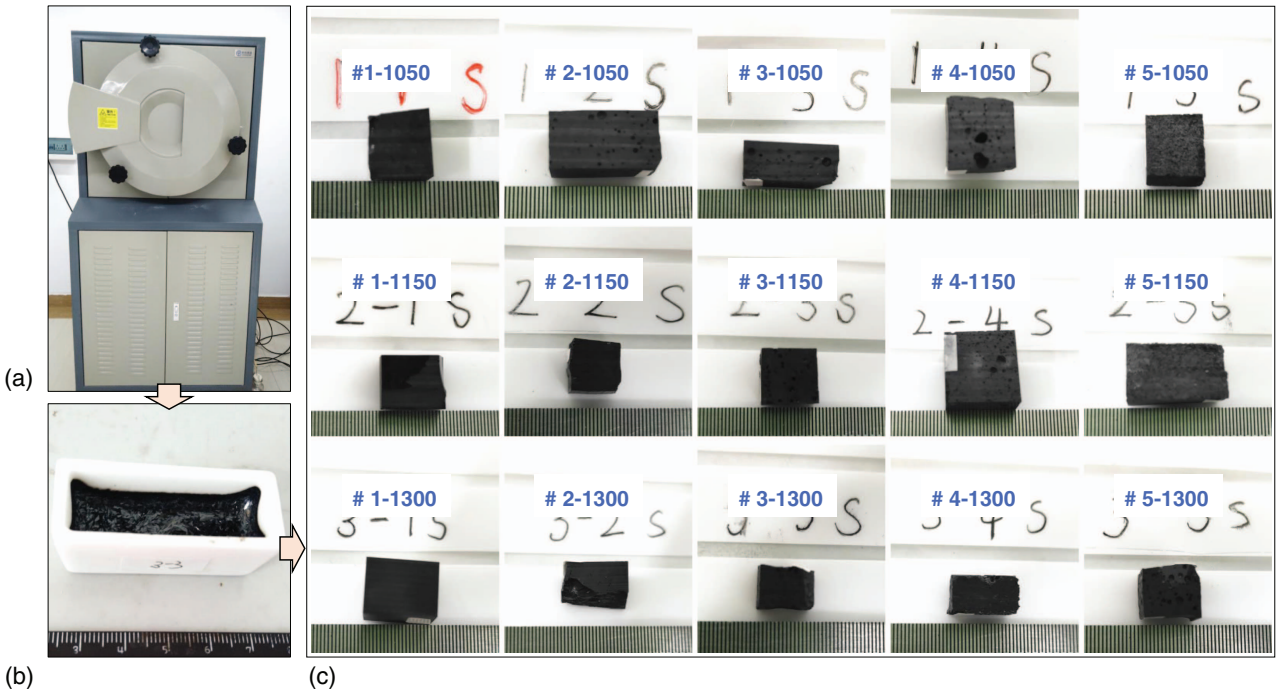

Fig. 1. (Color) Images of the studied samples: (a) microwave high-temperature furnace (CY-AT1700C-M); (b) example of the sintered lunar regolith stimulant; and (c) 15 sintered products for the prepared ilmenite-bearing regolith simulants at different sintering temperatures (i.e., 1,050°C, 1,150°C, and 1,300°C).

J. Aerosp. Eng., 2021, 34(6): 06021006

Downloaded from ascelibrary.org by TSINGHUA UNIVERSITY on 11/28/21. Copyright ASCE. For personal use only; all rights reserved.

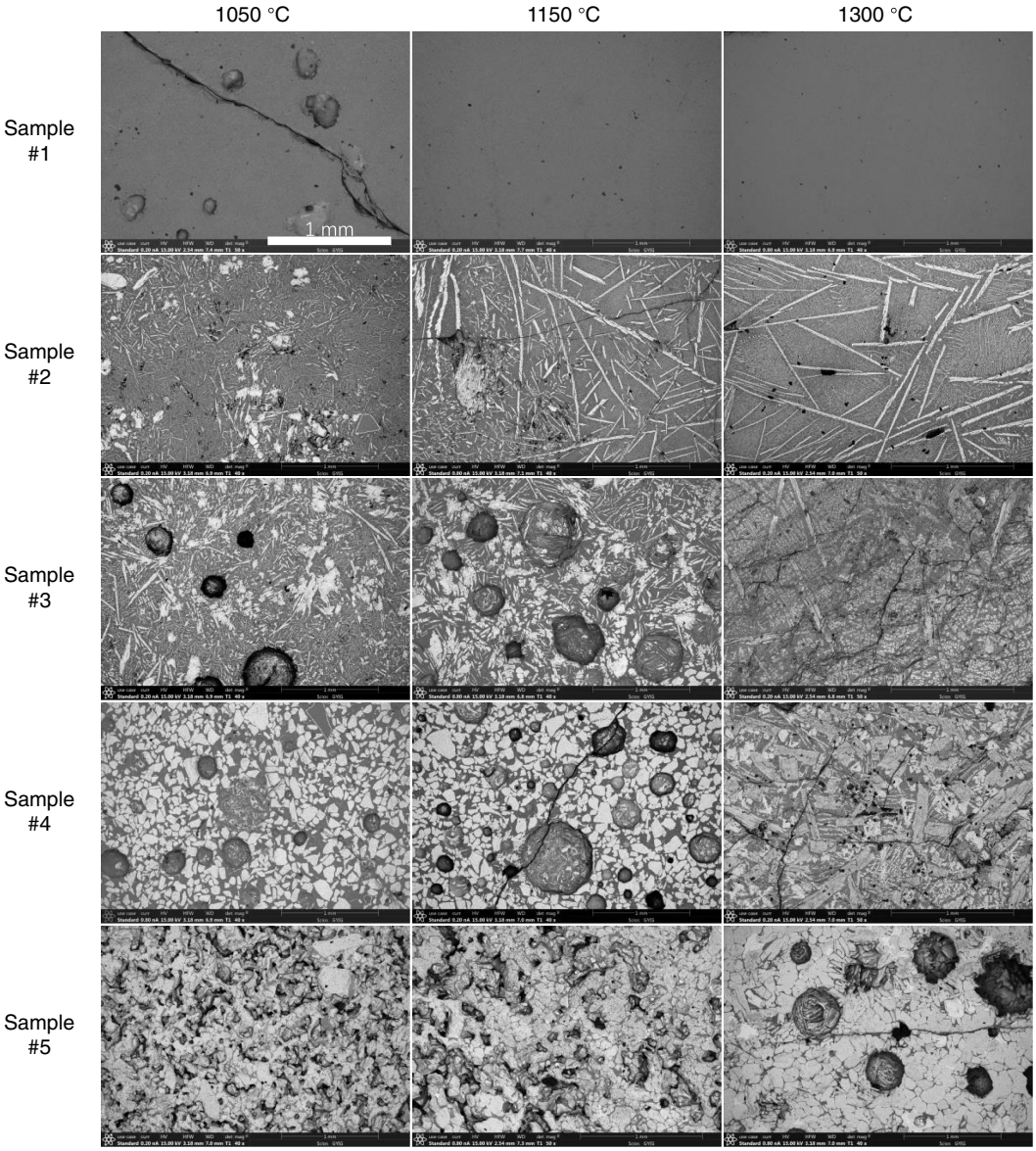

Fig. 2. Representative BSE images of the 15 sintered products with different contents of ilmenite and sintering temperatures (i.e., 1,050°C, 1,150°C, and 1,300°C).

minerals underwent little change (Fig. 3). There was a large amount of glass in the sintered products compared with that of the samples before sintering. The products from the samples with 4.6% by weight ilmenite sintered at 1,150°C and 1,300°C consisted almost entirely of glass, whereas other products contained pyroxene, olivine, Fe-Ti oxides, and glass. This means that ilmenite, with its good microwave absorption capability, may affect the recrystallization of silicate minerals during high-temperature microwave sintering.

Some of the ilmenite decomposed into pseudobrookite after the microwave sintering, and the amount of decomposed ilmenite increased with increasing sintering temperatures. The reaction can be expressed as follows:

$$4FeTiO_3 + O_2 \rightarrow 2Fe_2TiO_5 + 2TiO_2 \quad (1)$$

A potential reason for the oxidation reaction in ilmenite may be the presence of residual oxygen in the powder sample or/and the additional oxidation condition produced during the melting of silicate mineral. Considering the oxygen fugacity has a large influence on the stability of the Fe-Ti oxides, small amount of oxygen can cause the reaction with ilmenite (Toplis and Carroll 1995). In addition, the pseudobrookite may also be closely linked to the disproportionation of ferrous iron in ilmenite (Williams et al. 2012). The behavior of ilmenite at high temperature is very complicated and requires further research in the future.

In combination with the microstructure, the sintered products from the samples with 4.6% by weight ilmenite were relatively dense with less pores and cracks, which was consistent with the products, and almost entirely composed of glass. When the content of ilmenite increased, the glass content of the products decreased, and the cracks and pores of the products increased correspondingly, which affected the uniformity and density of the sintered products. The samples with low ilmenite content and microwave-sintered at high temperature could completely melt and form uniform silicate glass, which improved their compactness.

Thermal Conductivity

The thermal properties of the materials, especially the thermal conductivity, significantly affect the thermal insulation performance of

Downloaded from ascelibrary.org by TSINGHUA UNIVERSITY on 11/28/21. Copyright ASCE. For personal use only; all rights reserved.

Downloaded from ascelibrary.org by TSINGHUA UNIVERSITY on 11/28/21. Copyright ASCE. For personal use only; all rights reserved.

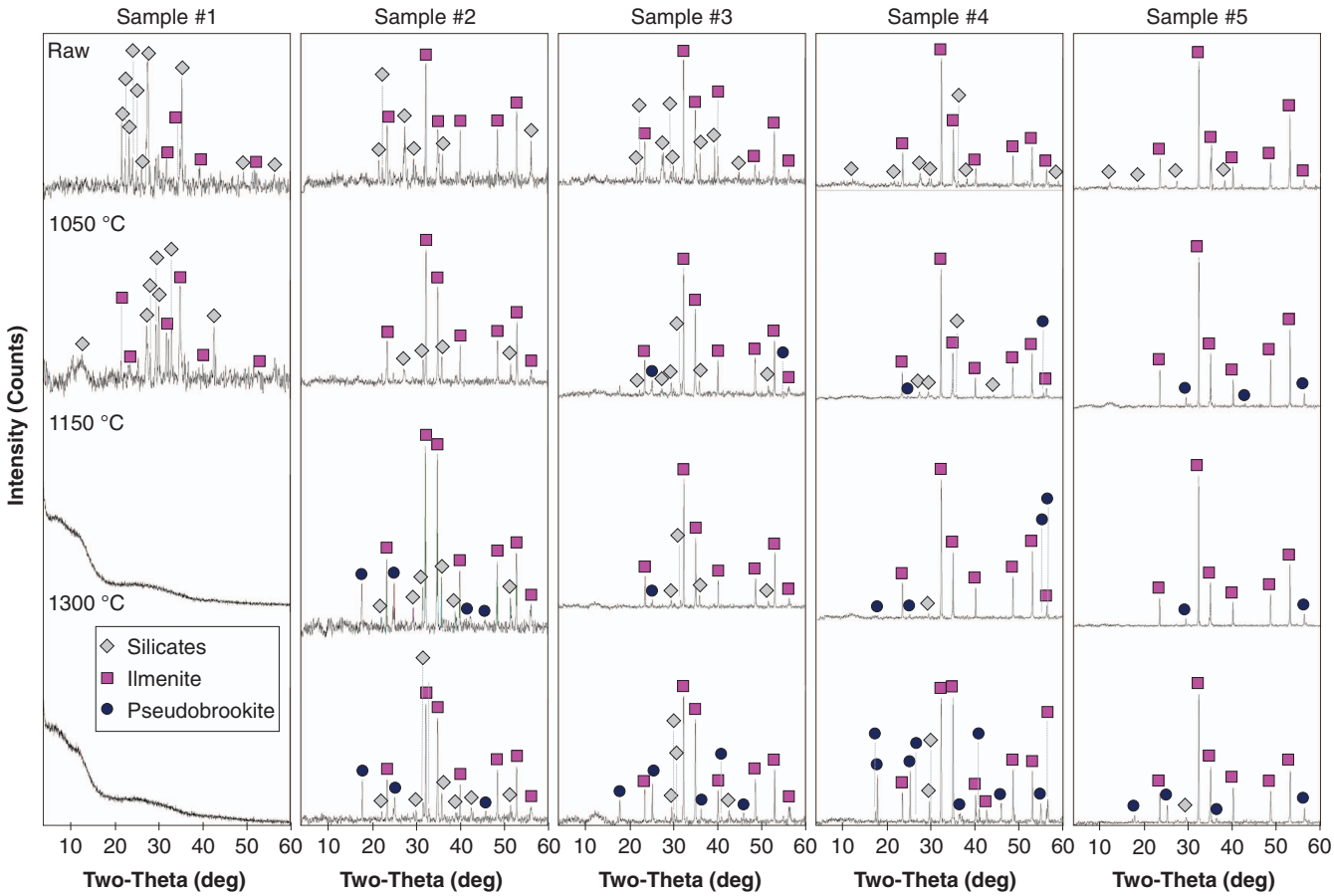

Fig. 3. (Color) XRD patterns for the five prepared regolith simulants and 15 sintered products.

lunar base structures. Fig. 4 shows the thermal conductivity of powder samples before sintering and sintered products after sintering. The results show that (1) as the ilmenite content increased, the thermal conductivity of the powder samples generally increased, 2)) compared with the powder samples, the thermal conductivity of the sintered products noticeably increased, (3) the thermal conductivity of the sintered products ranged from 0.1 ± 0.003 to 0.2 ± 0.006 W m^{-1} K^{-1}, approximately an order of magnitude higher than that of the powder samples, (4) the thermal conductivity decreased with sintering temperature, except for that of products from samples with 43.9% by weight ilmenite sintered at 1,050°C and 1,150°C, and (5) the effect of the ilmenite content on the thermal conductivity of the products was noticeable at different temperatures. At 1,050°C and 1,150°C, the thermal conductivity of the products first increased and then decreased with the increase of the ilmenite content. The thermal conductivity of the products decreased as the ilmenite content increased, and finally increased at 1,300°C.

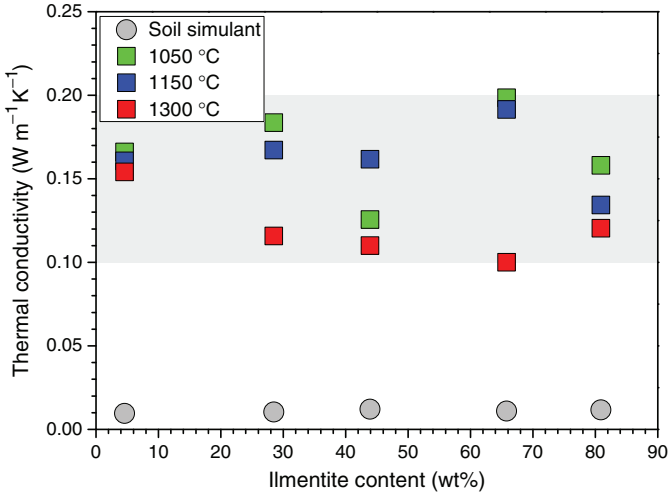

Fig. 4. (Color) Thermal conductivity of the powered regolith simulants (gray circles) and the sintered products at different temperatures (color squares).

Compressive Strength

Based on the compressive strength experiments, the compressive strength of the sintered products ranged from 12.5 ± 0.7 to 74.0 ± 7.1 MPa and exhibited a general decreasing trend with an increase in the ilmenite content (Fig. 5). In general, there was no evident correlation between the compressive strength of the sintered products and sintering temperature, whereas the sintered products from samples with 4.6% by weight ilmenite displayed an increase in compressive strength with the increase of temperature.

Implications for the ISRU of Lunar Regolith

There are several problems regarding to the establishment of a lunar base supporting long-term human habitation, including (1) suitable protection against the extreme lunar environment (e.g., radiation, micrometeoroids, and harsh thermal environment) must be provided, and (2) the in situ utilization of lunar regolith as a building material must be examined from an economic viewpoint. The easily accessed regolith, which has the potential to be directly

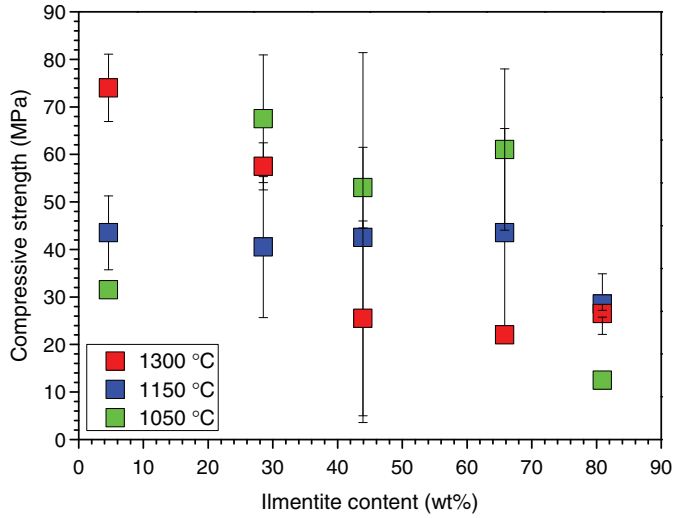

Fig. 5. (Color) Compressive strength of the sintered products.

heated in situ, makes microwave sintering a potential method for producing solid structures (Allan et al. 2013). The properties of microwave-sintered lunar regolith products, including microstructure, mineralogy, thermal performance, and mechanical properties, are important for evaluating the viability of microwave sintering technology on the Moon.

The microwave sintering experiments of lunar regolith simulant CLRS-1 with different ilmenite contents produced solid structural materials. The comparison of microstructure, mineralogy, thermal insulation, and mechanical properties of the sintered products indicates that the product from the sample with 4.6% by weight ilmenite sintered at 1,300°C showed superior performance. Due to the low ilmenite content, the silicate minerals in the sample sintered at high temperature completely melted and formed an entirely glassy product. The product had a compact and uniform microstructure with few visible pores and cracks and possessed a maximum compressive strength of up to 74.0 ± 7.1 MPa. By comparison, the compressive strength of this product is much greater than that of the products obtained by microwave sintering by Meek et al. (1987) and Allen et al. (1994) (i.e., 5–25 and ~7.6 MPa, respectively). Compared with the high-quality MU30 ordinary sintered brick (with a compressive strength of ~30 MPa) for terrestrial construction, the sintering product in this study shows sufficient compressive strength (74.0 ± 7.1 MPa) to be used as a construction material for a lunar base.

The temperature on the Moon varies significantly (between 100 and 400 K in a lunar day) (Williams et al. 2017), which requires structural materials with good thermal insulation properties. Porous materials with low thermal conductivity generally have better insulation. The thermal conductivity of products with the best insulation performance in this study was 0.1 ± 0.003 W m^{-1} K^{-1}, which is lower than that of the sintered products (i.e., 0.265 W m^{-1} K^{-1}) produced under vacuum by Song et al. (2019). This value is also much lower than that of the product obtained by a high-temperature quenching experiment of JSC-1A [i.e., 2.0 ± 0.3 W m^{-1} K^{-1} (Pinheiro et al. 2013)]. This work demonstrates that microwave-sintered products have better thermal performance than products prepared by other methods (e.g., electrothermal sintering), making the microwave sintering technique promising for the preparation of structural materials for lunar bases.

Ilmenite in lunar regolith varies between 0% and 20% by weight and is mainly distributed in mare regions of the Moon (Lucey 1998; Lemelin et al. 2013). This mineral has a significant effect on the product properties of microwave-sintered lunar regolith simulants. In this study, the sintered products from samples with a low ilmenite content have optimal mechanical properties and thermal performance. This indicates that lunar low-Ti regolith is particularly suitable for the preparation of structural materials.

Conclusion

This work investigated the effect of the ilmenite content and sintering temperature on the properties of microwave-sintered lunar regolith simulants. The products were prepared by microwave sintering samples with ilmenite contents of 4.6%, 28.5%, 43.9%, 65.8%, and 80.9% by weight at temperatures of 1,050°C, 1,150°C, and 1,300°C. Measurements of microstructure, mineralogy, thermal conductivity, and compressive strength of the sintered products indicated that ilmenite content and sintering temperature have a significant influence on their properties. The product from the sample with 4.6% by weight ilmenite, which was sintered at 1,300°C, demonstrated superior performance. Specifically, this product was almost entirely composed of glass and had a dense structure with few visible pores and cracks. It had good thermal insulation properties (i.e., with thermal conductivity of 0.15 ± 0.005 W m^{-1} K^{-1}) and optimal compressive strength (i.e., 74.0 ± 7.1 MPa).

The results of this study show that structural materials with good thermal insulation and superior mechanical properties could be directly prepared by in situ microwave sintering of lunar regolith at high temperature. The parameters of the microwave sintering experiments in this work could be helpful for the future preparation of structural materials on the Moon. However, the high-vacuum environment on the lunar surface could have a significant effect on the sintering process and the properties of the sintered products (Meurisse et al. 2017). In the future, it is necessary to conduct microwave sintering of lunar regolith simulants in vacuum.

Data Availability Statement

Some or all data, models, or code that support the findings of this study are available from the corresponding author upon reasonable request.

Acknowledgments

This work was funded by the Strategic Priority Research Program of the Chinese Academy of Sciences (XDB 41000000), National Natural Science Foundation of China (Nos. 41773066 and 41931077), Youth Innovation Promotion Association CAS (2018435), preresearch project on Civil Aerospace Technologies by CNSA (D020201), the Open Research Fund of the Key Laboratory of Space Manufacturing Technology, Chinese Academy of Sciences (CAS-SMT-201901), Key Research Program of Frontier Sciences (QYZDY-SSW-DQC028), and Beijing Municipal Science and Technology commission (Z181100002918003). The authors would like to thank Xiandi Zeng, Hao Peng, Xu Ren, and Jiao Xu for their technical support.

References

Allan, S., J. Braunstein, I. Baranova, N. Vandervoort, M. Fall, and H. Shulman. 2013. "Computational modeling and experimental microwave processing of JSC-1a lunar simulant." *J. Aerosp. Eng.* 26 (1): 143–151. https://doi.org/10.1061/(ASCE)AS.1943-5525.0000245.

Downloaded from ascelibrary.org by TSINGHUA UNIVERSITY on 11/28/21. Copyright ASCE. For personal use only; all rights reserved.

Allen, C. C. 1998. *Bricks and ceramics*. LPI Technical Rep. No. 98-01. Houston: Lunar and Planetary Institute.
Allen, C. C., J. C. Graf, and D. S. McKay. 1994. "Sintering bricks on the Moon." In *Proc., Engineering, Construction, and Operations in Space IV*, 1220–1229. New York: ASCE.
Allen, C. C., J. A. Hines, D. A. Altemir, and D. S. Mckay. 1992. "Sintering of lunar simulant basalt." In Vol. 23 of *Proc., Lunar and Planetary Science Conf.*, 19–20. Houston: Lunar and Planetary Institute.
Altemir, D. A. 1993. "Cold press sintering of simulated lunar basalt." In Vol. 24 of *Proc., Lunar and Planetary Science Conf.*, 23–24. Houston: Lunar and Planetary Institute.
Balla, V. K., L. B. Roberson, G. W. O'Connor, S. Trigwell, S. Bose, and A. Bandyopadhyay. 2012. "First demonstration on direct laser fabrication of lunar regolith parts." *Rapid Prototyping J.* 18 (Sep): 451–457. https://doi.org/10.1108/13552541211271992.
Cardiff, E. H., and B. C. Hall. 2008. "A dust mitigation vehicle utilizing direct solar heating." In *Proc., Joint Annual Meeting of Lunar Exploration Analysis Group-Int. Conf. on Exploration and Utilization of the Moon-Space Resources Roundtable (LEAG-ICEUM-SRR)*. Houston: Lunar and Planetary Institute.
Ceccanti, F., E. Dini, X. De Kestelier, V. Colla, and L. Pambaguian. 2010. "3D printing technology for a moon outpost exploiting lunar soil." In Vol. 3 of *Proc., 61st Int. Astronautical Congress (IAC-10-D3)*, 1–9. Noordwijk, Netherlands: European Space Agency.
Crawford, I. A. 2015. "Lunar resources: A review." *Prog. Phys. Geogr.* 39 (2): 137–167. https://doi.org/10.1177/0309133314567585.
Deng, Y.-F., X.-Y. Song, P. Hollings, L.-M. Chen, T. Zhou, F. Yuan, W. Xie, D. Zhang, and B. Zhao. 2017. "Lithological and geochemical constraints on the magma conduit systems of the Huangshan Ni-Cu sulfide deposit, NW China." *Miner. Deposita* 52 (6): 845–862. https://doi.org/10.1007/s00126-016-0703-7.
Duke, M. B., B. R. Blair, and J. Diaz. 2003. "Lunar resource utilization: Implications for commerce and exploration." *Adv. Space Res.* 31 (11): 2413–2419. https://doi.org/10.1016/S0273-1177(03)00550-7.
Faierson, E. J., and K. V. Logan. 2012. "Potential ISRU of lunar regolith for planetary habitation applications." In *Moon*, 201–234. Berlin: Springer.
Fateri, M., et al. 2019. "Solar sintering for lunar additive manufacturing." *J. Aerosp. Eng.* 32 (6): 04019101. https://doi.org/10.1061/(ASCE)AS.1943-5525.0001093.
Fateri, M., and A. Gebhardt. 2015. "Process parameters development of selective laser melting of lunar regolith for on-site manufacturing applications." *Int. J. Appl. Ceram. Technol.* 12 (1): 46–52. https://doi.org/10.1111/ijac.12326.
Fateri, M., A. Gebhardt, and M. Khosravi. 2013. "Experimental investigation of selective laser melting of lunar regolith for in-situ applications." In Vol. 56185 of *Proc., ASME Int. Mechanical Engineering Congress and Exposition*, V02AT02A008. New York: ASME.
Hill, E., L. A. Taylor, Y. Liu, and J. M. D. Day. 2005. "Microwave processing of lunar soil simulants JSC-1 and MLS-1." In Vol. 40 of *Proc., 68th Annual Meteoritical Society Meeting*. Chantilly, VA: Meteoritical Society.
Kalapodis, N., G. Kampas, and O.-J. Ktenidou. 2020. "A review towards the design of extraterrestrial structures: From regolith to human outposts." *Acta Astronaut.* 175 (Oct): 540–569. https://doi.org/10.1016/j.actaastro.2020.05.038.
Lemelin, M., C.-E. Morisset, M. Germain, V. Hipkin, K. Goïta, and P. G. Lucey. 2013. "Ilmenite mapping of the lunar regolith over Mare Australe and Mare Ingenii regions: An optimized multisource approach based on Hapke radiative transfer theory." *J. Geophys. Res.: Planets* 118 (12): 2582–2593. https://doi.org/10.1002/2013JE004392.
Lim, S., J. Bowen, G. Degli-Alessandrini, M. Anand, A. Cowley, and V. L. Prabhu. 2021. "Investigating the microwave heating behaviour of lunar soil simulant JSC-1A at different input powers." *Sci. Rep.* 11 (1): 1–16. https://doi.org/10.1038/s41598-021-81691-w.
Lim, S., V. L. Prabhu, M. Anand, and L. A. Taylor. 2017. "Extra-terrestrial construction processes—Advancements, opportunities and challenges." *Adv. Space Res.* 60 (7): 1413–1429. https://doi.org/10.1016/j.asr.2017.06.038.
Lucey, P., et al. 2006. "Understanding the lunar surface and space-Moon interactions." *Rev. Mineral. Geochem.* 60 (1): 83–219. https://doi.org/10.2138/rmg.2006.60.2.
Lucey, P. G. 1998. "Model near-infrared optical constants of olivine and pyroxene as a function of iron content." *J. Geophys. Res.: Planets* 103 (E1): 1703–1713. https://doi.org/10.1029/97JE03145.
Meek, T. T., D. T. Vaniman, R. D. Blake, and M. J. Godbole. 1987. "Sintering of lunar soil simulants using 2.45 GHz microwave radiation." In Vol. 18 of *Proc., Lunar and Planetary Science Conf.*, 635–636. Houston: Lunar and Planetary Institute.
Meek, T. T., D. T. Vaniman, F. H. Cocks, and R. A. Wright. 1984. "Microwave processing of lunar materials: Potential applications." In *Lunar bases and space activities of the 21st century*, 479–486. Houston: Lunar and Planetary Institute.
Meurisse, A., J. C. Beltzung, M. Kolbe, A. Cowley, and M. Spert. 2017. "Influence of mineral composition on sintering lunar regolith." *J. Aerosp. Eng.* 30 (4): 04017014. https://doi.org/10.1061/(ASCE)AS.1943-5525.0000721.
Nakamura, T., and B. K. Smith. 2005. "Solar thermal power system for lunar ISRU processes." In *Proc. SPIE 13 81240B–81240B*. College Park, MD: American Institute of Physics.
Pinheiro, A. S., Z. M. da Costa, M. J. V. Bell, V. Anjos, S. T. Reis, and C. S. Ray. 2013. "Thermal characterization of glasses prepared from simulated compositions of lunar soil JSC-1A." *J. Non-Cryst. Solids* 359 (Jan): 56–59. https://doi.org/10.1016/j.jnoncrysol.2012.09.027.
Rousek, T., K. Eriksson, and O. Doule. 2012. "SinterHab." *Acta Astronaut.* 74 (May): 98–111. https://doi.org/10.1016/j.actaastro.2011.10.009.
Ruess, F., J. Schaenzlin, and H. Benaroya. 2006. "Structural design of a lunar habitat." *J. Aerosp. Eng.* 19 (3): 133–157. https://doi.org/10.1061/(ASCE)0893-1321(2006)19:3(133).
Sato, H., M. S. Robinson, S. J. Lawrence, B. W. Denevi, B. Hapke, B. L. Jolliff, and H. Hiesinger. 2017. "Lunar mare TiO_2 abundances estimated from UV/Vis reflectance." *Icarus* 296 (Nov): 216–238. https://doi.org/10.1016/j.icarus.2017.06.013.
Song, L., J. Xu, S. Fan, H. Tang, X. Li, J. Liu, and X. Duan. 2019. "Vacuum sintered lunar regolith simulant: Pore-forming and thermal conductivity." *Ceram. Int.* 45 (3): 3627–3633. https://doi.org/10.1016/j.ceramint.2018.11.023.
Song, L., J. Xu, H. Tang, J. Liu, J. Liu, X. Li, and S. Fan. 2020. "Vacuum sintering behavior and magnetic transformation for high-Ti type basalt simulated lunar regolith." *Icarus* 347 (Sep): 113810. https://doi.org/10.1016/j.icarus.2020.113810.
Taylor, L. A., and T. T. Meek. 2005. "Microwave sintering of lunar soil: Properties, theory, and practice." *J. Aerosp. Eng.* 18 (3): 188–196. https://doi.org/10.1061/(ASCE)0893-1321(2005)18:3(188).
Taylor, S. L., A. E. Jakus, K. D. Koube, A. J. Ibeh, N. R. Geisendorfer, R. N. Shah, and D. C. Dunand. 2018. "Sintering of micro-trusses created by extrusion-3D-printing of lunar regolith inks." *Acta Astronaut.* 143 (Feb): 1–8. https://doi.org/10.1016/j.actaastro.2017.11.005.
Temple, D. G., M. T. Goff, J. D. Martin, D. Agresti, and W. W. Boles. 2006. "Microwave induced carbothermic reduction of iron oxides in lunar soil simulant." In *Proc., Earth & Space 2006: Engineering, Construction, and Operations in Challenging Environment*, 1–6. Reston, VA: ASCE.
Toplis, M. J., and M. R. Carroll. 1995. "An experimental study of the influence of oxygen fugacity on Fe-Ti oxide stability, phase relations, and mineral—melt equilibria in ferro-basaltic systems." *J. Petrol.* 36 (5): 1137–1170. https://doi.org/10.1093/petrology/36.5.1137.
Vaniman, D. T., T. T. Meek, and R. D. Blake. 1986. "Fusing lunar materials with microwave energy. Part II: Melting of a simulated glassy Apollo 11 soil." In *Proc., Lunar and Planetary Science Conf.*, 911–912. Houston: Lunar and Planetary Institute.
Williams, H. M., B. J. Wood, J. Wade, D. J. Frost, and J. Tuff. 2012. "Isotopic evidence for internal oxidation of the Earth's mantle during accretion." *Earth Planet. Sci. Lett.* 321 (Mar): 54–63. https://doi.org/10.1016/j.epsl.2011.12.030.
Williams, J. P., D. A. Paige, B. T. Greenhagen, and E. Sefton-Nash. 2017. "The global surface temperatures of the Moon as measured by the diviner lunar radiometer experiment." *Icarus* 283 (Feb): 300–325. https://doi.org/10.1016/j.icarus.2016.08.012.

Downloaded from ascelibrary.org by TSINGHUA UNIVERSITY on 11/28/21. Copyright ASCE. For personal use only; all rights reserved.

Wright, R. A., F. H. Cocks, D. T. Vaniman, R. D. Blake, and T. T. Meek. 1986. "Fusing lunar materials with microwave energy. Part I: Studies of doping media." In *Proc., Lunar and Planetary Science Conf.*, 958–959. Houston: Lunar and Planetary Institute.

Xu, J., X. Sun, H. Cao, H. Tang, H. Ma, L. Song, X. Li, X. Duan, and J. Liu. 2019. "3D printing of hypothetical brick by selective laser sintering using lunar regolith simulant and ilmenite powders." In Vol. 10842 of *Proc., 9th Int. Symp. on Advanced Optical Manufacturing and Testing Technologies: Subdiffraction-Limited Plasmonic Lithography and Innovative Manufacturing Technology*, 1084208. Beijing: Chinese Optical Society.

Zheng, Y., S. Wang, Z. Ouyang, Y. Zou, J. Liu, C. Li, X. Li, and J. Feng. 2009. "CAS-1 lunar soil simulant." *Adv. Space Res.* 43 (3): 448–454. https://doi.org/10.1016/j.asr.2008.07.006.

Zhou, C., R. Chen, J. Xu, L. Ding, H. Luo, J. Fan, E. J. Chen, L. Cai, and B. Tang. 2019. "In-situ construction method for lunar habitation: Chinese Super Mason." *Autom. Constr.* 104 (Aug): 66–79. https://doi.org/10.1016/j.autcon.2019.03.024.

Downloaded from ascelibrary.org by TSINGHUA UNIVERSITY on 11/28/21. Copyright ASCE. For personal use only; all rights reserved.